Computer Assisted Mechanics and Engineering Sciences, 2: 307–319, 1995.
Copyright © 1995 by Polska Akademia Nauk

Numerical modelling of thermal waves via internal state variable approach

Czesław Bajer and Witold Kosiński
Institute of Fundamental Technological Research, Polish Academy of Sciences
ul. Świętokrzyska 21, 00-049 Warsaw, Poland

(Received April 10, 1995)

Numerical solutions by means of the space–time finite element method to initial-boundary value problems for a hyperbolic model of heat conduction, are obtained. The heat conduction description is based on a concept a rigid conductor with a scalar internal state variable, that leads to a modified Fourier law. The obtained results are compared with existing experimental data know for semi-conductor crystals at low temperature.

1. INTRODUCTION

It is well known that the simple dependence of energy ψ^* on thermodynamic (absolute) temperature ϑ and the classical Fourier law combined with the first and second laws of thermodynamics lead to the heat conduction equation of the parabolic (nonlinear) type. Unfortunately, the same result will be obtained if under the function symbol ψ^* the temperature gradient $\nabla\vartheta$ appears.

To modify heat conduction equation and to get a finite speed of propagation of any thermal disturbances, the constitutive equation for the energy must be changed.

Various types of hyperbolic heat conduction equations leading to finite speed of thermal wave propagation were postulated for rigid and deformable heat conductors in the last four decades. After Maxwell [35] and Landau's model for fluids, Cattaneo [15, 16], Vernotte [41] and Chester [17] for rigid conductors, one can find dozens of papers in which different approaches have been used to model second sound effect observed in solids (cf. [37, 39]).

In the paper the concept of a scalar internal state variable, playing a role of the so-called *semi-empirical temperature scale*, different from the absolute, is introduced. Then its gradient gives the direction of the heat flux vector, while the proportionality coefficient depends on the absolute temperature. In the constructed model one requires three experimental curves, namely the specific heat, thermal conductivity coefficient (called here the equilibrium heat conduction coefficient) and second sound speed (i.e. speed of thermal disturbances), all given in terms of the absolute temperature, determine the model. In this respect the present model has a common part with the model developed independently by Morro and Ruggeri [36] in the framework of the extended thermodynamics.

The model of heat conduction developed leads to a system of two scalar equations: one is of the second order in the scalar internal state variable and of the first order in the absolute temperature. The second equation is of the first order. The system is of the hyperbolic type with two non-vanishing characteristic velocities, giving a finite thermal wave speeds. The main aim of the paper is to model numerically the derived system of equations.

Conventional numerical methods applied to date imply separate discretization of the differential equation in space and in time. Finite differences or finite elements are applied to spatial derivatives while Runge-Kutta, Newmark or simply — central differences are commonly used in the time integration of time derivatives. However, in such an approach, when interpolation over space and

time is carried out by using decoupled interpolation formulas, all the equations of equilibrium are fulfilled only in discrete time t_i. Thus discontinuous in time distribution of parameters is implemented. It disables sufficiently accurate investigation of quantities that vary considerably between time levels.

Our formulation of the problem leads to a non-linear equation, in which certain parameters strongly depend on the temperature. In such a case numerical solution obtained can be disturbed by numerical errors (mainly approximation errors). That is why our wish is to use the method which would enable mesh modification in order to reduce the discretization error. In classical approaches spatial mesh modification can only be done by re-meshing techniques. Here we would like to propose the approximation continuous in space and time of unknown parameters by using the space–time finite element method. The numerical method was especially chosen for the solution to enable further applications with non-stationary spatial partition, i.e. domain evolution, phase change, mesh adaptation with discretization error reduction. In the present paper only the simplest particular case with constant mesh will be applied. In such a case the approach is similar to the group of classical time integration schemes.

First attempts of the space–time modelling of physical problems were published in [23, 24]. The definition of the minimized functional allowed to derive the relation between the time variable and spatial variables in space–time subdomains. Oden [38] proposed a general approach to the finite element method. He extended the image of the discretized structure on time variable. Unfortunately, this interesting idea of the non-stationary partition of the structure on subspaces proposed has not been continued. Argyris, Scharpf, Chan and Fried [1, 2, 3, 21] have formulated problems with space and time treated equally. However, in the papers of Kuang and Atluri, for example [34], the final discretization was carried on separately for time and space.

Independently of the researches mentioned above Kączkowski in his papers [27, 28] introduced for the first time some abstract physical terms to mechanics: an equation of time–work, mass as a vector quantity or a space–time rigidity. A synthesis of the space–time element method can be found in [29, 11] while stability considerations in [5]. Space–time elements which lead to unconditionally stable solution schemes were described in [26]. Unfortunately they could be only applied for space–time forms rectangular in time, obtained as a vector product of a spatial domain and a time interval. In next papers some authors turned to non-rectangular shapes of elements. Then a non-stationary partition of the structure and non-rectangular space–time elements [4, 5, 13] enabled to solve a quite new group of problems by the space–time element method: contact problems [10], problems with adaptive mesh [4, 6, 9], problems of evolution [7, 8, 14].

In our approach we assume that in the time interval $[t_i;\ t_i + h]$ both the investigated parameters and the geometry of the discrete mesh can vary continuously in time. The technique is similar to the moving mesh technique, that was successfully applied to parabolic problems (for example [42]). Unfortunately, hyperbolic problems were rarely treated in that way. We will try to apply a full space–time discretization to our hyperbolic problem.

2. MODEL WITH SEMI-EMPIRICAL TEMPERATURE

Recently in a series of papers [18, 19, 30–32] a thermodynamic, phenomenological theory of heat conduction with finite wave speed has been developed and applied to thermal wave propagation problems (mostly 1D); the well-posedness of a Cauchy problem has been demonstrated also [20]. The theory is based on the concept of a gradient generalization of the internal state variable approach [33], in which the gradient of a scalar internal state variable (called a semi-empirical temperature) β influences the response of the material at hand. β represents the history of the temperature. It cannot be directly measured. Here it can be considered as a potential, with the analogy to the classical heat conduction Fourier law. There the heat flux is proportional to the temperature gradient, here the heat flux is proportional to the gradient of β. At a typical particle X

of a medium under consideration the internal state variable is a solution of an initial value problem

$$\dot{\beta} = F(\vartheta, \beta), \quad \beta(t_0) = \beta_0, \tag{1}$$

where ϑ is the absolute (thermodynamic) temperature at X and the superposed dot denotes the differentiation with respect to time t. The material function F depends on thermal properties of the medium at hand, e.g. conductivity, and on some time interval τ characteristic for the thermal inertia.

In further constitutive modelling one assumes, after Cattaneo [15, 16], that both relations: the classical Fourier law of heat conduction

$$\mathbf{q} = -k\nabla\vartheta, \tag{2}$$

with $k(\vartheta)$ as an equilibrium heat conduction coefficient and the temperature gradient $\nabla\vartheta$, as well as the differential relation derived for the heat flux $\mathbf{q}$ from Eq. (1) (due to a particular constitutive equations for the free energy) play the role of balance equations, however, with different approximations of the mean kinetic energy of molecules of the medium. This point of view, together with the statistical arguments given in [18], implies that instead of the temperature gradient the spatial gradient of the semi-empirical temperature, i.e. $\nabla\beta$, appears in the following constitutive relations, for the Helmholtz free energy ψ, specific entropy η and heat flux $\mathbf{q}$,

$$\begin{aligned} \psi &= \psi^*(\vartheta, \nabla\beta), \\ \eta &= \eta^*(\vartheta, \nabla\beta), \\ \mathbf{q} &= \mathbf{q}^*(\vartheta, \nabla\beta). \end{aligned} \tag{3}$$

Moreover, it is assumed that the Fourier law is to obtain if the thermal relaxation time τ vanishes; then β becomes a function of ϑ. This assumption is used in the derivation of the relations between material functions and the heat conduction coefficient $k(\vartheta)$ measured in classical experiments on heat conduction.

Since τ represents the time dimension parameter in F, and the both variables β and ϑ have the dimension of temperature (kelvin), the dimensional analysis implies the existence of a function f (of β and ϑ) of the dimension of temperature, such that

$$F(\vartheta, \beta) \equiv \tau^{-1} f(\vartheta, \beta). \tag{4}$$

Then the kinetic equation (1) takes the form

$$\tau\dot{\beta} = f(\vartheta, \beta) \tag{5}$$

and the limit case of vanishing τ corresponds to $f(\vartheta, \beta) = 0$, identically in ϑ and β. Hence in this case an algebraic relation between the both scales follows, provided the derivative $\frac{\partial f}{\partial \beta}$ is different from zero. Note that in the general case if that derivative is negative, for positive τ, then the stability of solutions of Eq. (5) is guaranteed.

In the case of an isotropic medium the second law of thermodynamics is satisfied [18, 19] if

$$\begin{aligned} &\mathbf{q} = -\alpha^* \nabla\beta, \\ &\eta = -\frac{\partial \psi^*}{\partial \vartheta}, \\ &\alpha^* \frac{\partial f}{\partial \beta} \left(\frac{\partial f}{\partial \vartheta}\right)^{-1} \leq 0, \end{aligned} \tag{6}$$

where

$$\alpha^* \equiv \frac{\rho\vartheta}{\tau} \frac{\partial f}{\partial \vartheta} \frac{\partial \psi^*}{\partial |\nabla\beta|} \frac{1}{|\nabla\beta|} \tag{7}$$

has the dimension of a thermal conductivity coefficient. Let us first notice that the coefficient α^* cannot depend on β, for the form of Eq. (3), and consequently the function f is governed by the equation

$$\frac{\partial^2 f}{\partial \vartheta \partial \beta} = 0 .$$

Thus the general form of f is

$$f(\vartheta, \beta) = f_1(\vartheta) + f_2(\beta) . \tag{8}$$

If one assumes that the relation between $\mathbf{q}$ and $\nabla\beta$ in Eqs. (6) is linear, then $\alpha^* = \alpha^*(\vartheta)$ and Eq. (7) can be regarded as a differential equation for ψ^* ; integrating it one gets

$$\psi = \psi_1^*(\vartheta) + 0.5\psi_2^*(\vartheta)|\nabla\beta|^2 , \tag{9}$$

where $\psi_1^*(\vartheta)$ plays the role of the classical free energy function and

$$\psi_2^*(\vartheta) = \frac{\tau\alpha^*(\vartheta)}{\rho\vartheta f_1'(\vartheta)} . \tag{10}$$

Here the prime denotes the differentiation with respect to the argument. Note that $\psi_2^*(\vartheta)$ vanishes when τ tends to zero. The last relation plays the role of a compatibility condition in the theory.

From Eqs. (6) the form of the entropy function η^* follows. Its form we shall write down after making the following simplified assumption, namely, the internal energy $\epsilon = \psi + \eta\vartheta$ is a function of ϑ only (i.e. independent of grad β). This assumption is compatible with several classical theories (e.g. the Debeye theory) and secures the specific heat to be a function of the absolute temperature only. Then, in view of Eqs. (6) and (9), necessarily $\psi_2^*(\vartheta)$ is a linear function of temperature

$$\psi_2^*(\vartheta) = \psi_{20}\vartheta . \tag{11}$$

The material coefficient ψ_{20} can be expressed in terms of the mass density ρ, the relaxation time τ and two other dimensional material constants: k_0 of the dimension of thermal conductivity coefficient and ϑ_0 of the dimension of temperature, with the help of the dimensional analysis [30] as follows

$$\psi_{20} = \frac{\tau k_0}{\rho\vartheta_0^2} . \tag{12}$$

The expression for the entropy follows from Eqs. (6), (9)–(11) as

$$\eta^*(\vartheta, \nabla\beta) = \eta_E(\vartheta) - 0.5\psi_{20}|\nabla\beta|^2 , \tag{13}$$

where the term $\eta_E(\vartheta) = -\psi_1^{*\prime}(\vartheta)$ represents the so-called conservative (equilibrium) entropy , while the second term — the non-equilibrium part. The later can be expressed as a second order term in $\frac{\mathbf{q}}{\alpha^*(\vartheta)}$ if the constitutive equation (6) will be used. Let us notice, that such a form of the entropy function is compatible with the principle of maximum at equilibrium (i.e. when $\mathbf{q}$ vanishes) provided ψ_{20} is non-negative [12]. However, due to the last inequality in (6) this requirement is equivalent to the non-positive derivative $\frac{\partial f}{\partial \beta}$, the later is related to the stability of solutions of the kinetic equation (5). Hence, we assume that the dimensional constant k_0 is positive.

It is worthwhile to mention, that the present model and the model developed by Morro and Ruggeri [36] will lead to the same solutions of field equations if the function $f_2(\beta)$ is linear, and the following identifications are made:

$$\alpha \equiv \frac{\tau}{\alpha^*(\vartheta)} \qquad \text{and} \qquad \nu \equiv f_1(\vartheta) , \tag{14}$$

where the material functions $\alpha(\vartheta)$ and $\nu(\vartheta)$ are those appearing in the extended thermodynamics model of Morro and Ruggeri [36], and provided initial conditions $(\vartheta(0), \mathbf{q}(0))$ of the second model will be adjusted to initial condition $(\beta(0), \vartheta(0))$ of the first model.

It should be pointed out that in the semi-empirical temperature model the identification of the function $f_2(\beta)$ can be made with the help of the equilibrium heat conduction coefficient k (cf. Eq. (19) in [19]).

Finally, let us notice that in the shock wave analysis performed in the second model [40] the form of the function $k(\vartheta)$, and consequently of $f_2(\beta)$ — for the first model — does not influence the results.

3. HEAT WAVE EQUATION

In this section we shall derive 3D equation that govern propagation of thermal waves in the model with the semi-empirical temperature. Let us substitute the constitutive equations (6–10) into the energy balance equation

$$\rho\dot{\epsilon} + \operatorname{div}\mathbf{q} = r\,, \tag{15}$$

where

$$\epsilon = \epsilon^*(\vartheta) = \psi^*(\vartheta, \nabla\beta) - \vartheta\frac{\partial\psi^*(\vartheta, \nabla\beta)}{\partial\vartheta}$$

is the specific internal energy and r denotes the rate of heat supply. Let us differentiate the kinetic equation (5) with respect to X and use the resulting prolongated equation to express all derivatives of ϑ in terms of the corresponding derivatives of β. Then we get

$$\tau\rho c_v(\vartheta)\ddot{\beta} - \tau\alpha^{*\prime}(\vartheta)\nabla\dot{\beta}\cdot\nabla\beta - \alpha^*(\vartheta)f_1'(\vartheta)\triangle\beta - \rho c_v(\vartheta)f_2'(\beta)\dot{\beta} + \alpha^{*\prime}(\vartheta)f_2'(\beta)\nabla\beta\cdot\nabla\beta = rf_1'(\vartheta)\,. \tag{16}$$

Here we have put $c_v(\vartheta) = \epsilon^{*\prime}(\vartheta)$ for the specific heat of the material at hand.

4. NUMERICAL APPROACH

The domain of observation is defined by

$$\Omega = \{(x,t)\colon\ x_L(t) \le x \le x_R(t),\ t_0 \le t < \infty\}\,. \tag{17}$$

$x_L(t)$ and $x_R(t)$ are functions that limit the spatial domain, for example moving boundary. They can be given explicitly or in a general case can depend on the solution. The domain Ω is divided into finite space–time elements. It cannot be done arbitrary. Some indications can be found in [5]. For each element characteristic matrices are calculated and a resulting matrix equation allows to solve the problem step-by-step.

We assume the rate $\dot{\beta}$ of the internal state variable β, called the semi-empirical temperature as an unknown quantity. In further considerations we take x and t as local variables in each subdomain.

Let us consider a time interval $[0, h]$. The distribution of the temperature within $[0, h]$ is described by the integral

$$\beta(t) = \beta_0 + \int_0^t \dot{\beta}\mathrm{d}t\,. \tag{18}$$

Second derivative $\ddot{\beta}$ and spatial derivative $\frac{\partial\beta}{\partial x}$ can be simply computed

$$\ddot{\beta} = \frac{\partial\dot{\beta}}{\partial t}\ , \tag{19}$$

$$\frac{\partial \beta}{\partial x} = \frac{\partial \beta(x,0)}{\partial x} + \frac{\partial}{\partial x}\left(\int_0^t \dot{\beta} \mathrm{d}t\right). \tag{20}$$

Let us multiply the governing equation (16) by virtual distribution of the semi-empirical temperature rate $\dot{\beta}^*$ and let us integrate the product over space and time $\Omega_e = \{(x,t) : 0 \leq x \leq b, 0 \leq t \leq h\}$. We assume here rectangular subdomains, for simplicity. In the other case we should integrate over trapezoidal domains Ω_e. Thus the equation of the virtual power is conduced to the equation of virtual work. Integration by parts will reduce the second derivative $\frac{\partial^2 \beta}{\partial x^2}$.

Now we can apply the interpolation formula for $\dot{\beta}$ in a form

$$\dot{\beta}(x,t) = \mathbf{N}(x,t)\,\mathbf{V} \tag{21}$$

The vector $\mathbf{V}$ is a set of nodal parameters and contains subvectors $\mathbf{V}_i$ and $\mathbf{V}_{i+1}$, i.e. solution vectors in two successive instants:

$$\mathbf{V} = \left\{ \begin{array}{c} \mathbf{V}_i \\ \mathbf{V}_{i+1} \end{array} \right\}. \tag{22}$$

$\mathbf{N}$ are interpolation functions in Ω_e. Relations (18), (19) and (20) can now be rewritten:

$$\beta(t) = \beta_0 + \int_0^t \mathbf{N} \mathrm{d}t \cdot \mathbf{V}, \tag{23}$$

$$\ddot{\beta} = \frac{\partial \mathbf{N}}{\partial t} \cdot \mathbf{V}, \tag{24}$$

$$\frac{\partial \beta}{\partial x} = \frac{\partial \beta(x,0)}{\partial x} + \frac{\partial}{\partial x}\left(\int_0^t \mathbf{N} \mathrm{d}t\right)\mathbf{V}. \tag{25}$$

Identical formulas can be written for β^*, $\dot{\beta}^*$, $\ddot{\beta}^*$ and $\frac{\partial \beta^*}{\partial x}$. In this case we use virtual interpolation functions $\mathbf{N}^*$ instead of $\mathbf{N}$. In the simplest case, as we mentioned before, we assume constant limits of Ω_e and then interpolation functions $\mathbf{N}$ are linear

$$\mathbf{N} = \left\{ \begin{array}{c} (1-\frac{x}{b})(1-\frac{t}{h}) \\ \frac{x}{b}(1-\frac{t}{h}) \\ (1-\frac{x}{b})\frac{t}{h} \\ \frac{x}{b}\frac{t}{h} \end{array} \right\}. \tag{26}$$

Our interpolation functions allow to fulfil the Neumann homogeneous conditions on the free end, if $h \to 0$.

Here the proper choice of distribution of the virtual velocity $\dot{\beta}^* = \mathbf{N}^*\mathbf{V}^*$ is the fundamental problem of the method on this stage. Convergence, efficiency, accuracy of the time integration and accuracy of the solution in the case of nonlinearities depend on the form of $\dot{\beta}^*$. The simplest one is the Dirac distribution with $\mathbf{V}^* = \mathbf{V}$.

$$\dot{\beta}^*(x,t) = \mathbf{N}^*\,\mathbf{V}^* = \mathbf{N}(x,h)\,\delta\left(\frac{t-t_i}{h} - \xi\right)\mathbf{V}, \qquad 0 \leq \xi \leq 1. \tag{27}$$

The product of the spatial interpolation function $\mathbf{N}$ determined for $t = t_{i+1}$ and the Dirac δ defines our virtual interpolation function $\mathbf{N}^*$. The form (27) is convenient for our purpose since it reduces the integration over the space and time to the integration over the space only. Moreover, it allows us to select the parameter ξ according to the stability condition. Other forms of virtual distribution are also possible [8]. However, we will reduce our consideration to the simplest single Dirac peak only.

Omitting $\mathbf{V}$ on the left hand side of each term we can write the discrete weak form of our equation (16)

$$\int_{\Omega_e} (\mathbf{N}^*)^T \tau \rho c_v(\vartheta) \frac{\partial \mathbf{N}}{\partial t} \mathbf{V} \, dx dt$$
$$- \int_{\Omega_e} (\mathbf{N}^*)^T \tau \alpha^{*\prime}(\vartheta) \frac{\partial \mathbf{N}}{\partial x} \mathbf{V} \left[\frac{\partial}{\partial x} \left(\int_0^t \mathbf{N} dt \right) \mathbf{V} + \frac{\partial \beta(x,0)}{\partial x} \right] dx dt$$
$$+ \int_{\Omega_e} \left(\frac{\partial \mathbf{N}^*}{\partial x} \right)^T \alpha^*(\vartheta) f_1'(\vartheta) \left[\frac{\partial}{\partial x} \left(\int_0^t \mathbf{N} dt \right) \mathbf{V} + \frac{\partial \beta(x,0)}{\partial x} \right] dx dt$$
$$+ \int_{\Omega_e} (\mathbf{N}^*)^T \frac{\partial}{\partial x} \left(\alpha^*(\vartheta) f_1'(\vartheta) \right) \left[\frac{\partial}{\partial x} \left(\int_0^t \mathbf{N} dt \right) \mathbf{V} + \frac{\partial \beta(x,0)}{\partial x} \right] dx dt$$
$$- \int_{\Omega_e} (\mathbf{N}^*)^T \rho c_v(\vartheta) f_2'(\beta) \mathbf{N} \mathbf{V} \, dx dt$$
$$- \int_{\Omega_e} (\mathbf{N}^*)^T \alpha^{*\prime}(\vartheta) f_2'(\beta) \left[\frac{\partial}{\partial x} \left(\int_0^t \mathbf{N} dt \right) \mathbf{V} + \frac{\partial \beta(x,0)}{\partial x} \right]^2 dx dt = \mathbf{R} . \tag{28}$$

$\mathbf{R}$ is the vector of the external heat impulses. In further considerations we assume it as equal to zero. We can apply our simple form of $\mathbf{N}^*$ to (28). Integration of (28) over time interval $[0, h]$ is simple since it is reduced to calculation of intermediate values. The resulting formula representing a weak form of the energy balance equation written for a single element has the form

$$(\mathbf{K}_{11} + \mathbf{K}_{21} + \mathbf{K}_{22} + \mathbf{K}_{31} + \mathbf{K}_{32} + \mathbf{K}_{41} + \mathbf{K}_{51} + \mathbf{K}_{52}) \mathbf{V} + \mathbf{L}_{31} + \mathbf{L}_{32} + \mathbf{L}_{51} = \mathbf{0} . \tag{29}$$

The first index corresponds to the place of the corresponding term in the differential equation (16). After assembling elemental matrices into a global one $\mathbf{K}$ and vectors into $\mathbf{L}$ for a whole domain, we have:

$$\mathbf{K} \mathbf{V} + \mathbf{L} = \mathbf{0} . \tag{30}$$

Here $\mathbf{K}$ has a dimension $N \times 2N$, where N is a number of degrees of freedom. Let us notice that $\mathbf{K}$ depends on the $\dot{\beta}$ and β through ϑ. The non-linear equation (30) is solved in each time interval iteratively. For this we need both $\dot{\beta}$ and β evaluated in $t = h$. Equation (30) can be expanded with respect to subvectors $\mathbf{V}_i$ and $\mathbf{V}_{i+1}$. For this let us split the matrix $\mathbf{K}$ (which is computed for a time interval $[t_i, t_{i+1}]$ and has the dimension $N \times 2N$) into square matrices $\mathbf{K}_i^L$ and $\mathbf{K}_i^R$.

$$\mathbf{K}_i^L \mathbf{V}_i + \mathbf{K}_i^R \mathbf{V}_{i+1} + \mathbf{L}_i = \mathbf{0} . \tag{31}$$

Now we have $\mathbf{V}$ in the step-by-step procedure

$$\mathbf{V}_{i+1} = -[\mathbf{K}_i^R]^{-1} (\mathbf{L}_i + \mathbf{K}_i^L \mathbf{V}_i) . \tag{32}$$

Now when we have the vector $\mathbf{V}_{i+1}$, which is the semi-empirical temperature rate vector received for time t_{i+1}, we can proceed with calculation of semi-empirical temperature vector $\mathbf{B}_{i+1}$. It is now the last unknown value we must determine to enable evaluation of all the coefficients of our fundamental equation. In the particular case of $\xi = \frac{1}{2}$ we can use the formula (23), in which $\mathbf{B}_{i+1}$ replaces $\beta(t)$ for $t = h$ and β_0 is replaced by $\mathbf{B}_i$. In such a case we have simple central difference formula for time derivative of β (represented by $\mathbf{V}$) written in time $t = t_i + \frac{h}{2}$. However, in our work we use a more general formulation for arbitrary ξ. That is why we modify the resulting form which will enable us to compute $\mathbf{B}_{i+1}$.

The average value of the velocity taken at time ηh, $0 \leq \eta \leq 1$ results in the formula

$$\mathbf{B}_{i+1} = \mathbf{B}_i + h [(1 - \eta) \mathbf{V}_i + \eta \mathbf{V}_{i+1}] . \tag{33}$$

The energy at the end of the time interval is preserved if $\eta = 1 - \xi$. Then we have finally

$$\mathbf{B}_{i+1} = \mathbf{B}_i + h [\xi \mathbf{V}_i + (1 - \xi) \mathbf{V}_{i+1}] . \tag{34}$$

It was proved in [7] that the unconditional stability of the process (32), (34) occurs for $\frac{\sqrt{2}}{2} \leq \xi \leq 1$. For $\xi = 1$ we have the explicit formula while for other values ($0 \leq \xi < 1$) the scheme is implicit and requires iterations to determine the geometry x_1.

Since we cannot precisely choose all the parameters in Eq. (16), especially to coincide the behavior of the mathematical model with the physical one, we will finally assume the following relations for f_1, f_2, ϑ, c_v and α^* [19]:

$$f_1(\vartheta) = \vartheta, \tag{35}$$

$$f_2(\beta) = -\beta, \tag{36}$$

$$\vartheta = \tau \frac{\partial \beta}{\partial t} + \beta, \tag{37}$$

$$c_v = c_{v0}\, \vartheta^3, \tag{38}$$

$$\alpha^* = \frac{\rho}{\tau} \psi_{20} \vartheta^2. \tag{39}$$

The integration of (28) over two dimensions is reduced to the integration over only the variable x. If we assume the coefficients α^*, $\alpha^{*\prime}$, c_v, f_1', f_1', to be constant in the spatial element, we can derive matrices $\mathbf{K}$ and vectors $\mathbf{L}$ in the explicit form. They are listed below for completion:

$$\mathbf{K}_{11} = \tau \rho\, c_{v0}\, \vartheta^3 \frac{b}{6h} \begin{bmatrix} -2 & -1 & 2 & 1 \\ -1 & -2 & 1 & 2 \end{bmatrix},$$

$$\mathbf{K}_{21} = -\rho \psi_{20} \vartheta \frac{h}{2b} [\xi - 1; -(\xi - 1); -\xi; \xi]\, \mathbf{V} \begin{bmatrix} \xi(\xi-2) & -\xi(\xi-2) & -\xi^2 & \xi^2 \\ \xi(\xi-2) & -\xi(\xi-2) & -\xi^2 & \xi^2 \end{bmatrix},$$

$$\mathbf{K}_{22} = -\rho \psi_{20} \vartheta \frac{\partial \beta(x,0)}{\partial x} \begin{bmatrix} \xi - 1 & -(\xi-1) & -\xi & \xi \\ \xi - 1 & -(\xi-1) & -\xi & \xi \end{bmatrix},$$

$$\mathbf{K}_{31} = \rho \psi_{20} \vartheta^2 \frac{h}{2\tau b} \begin{bmatrix} \xi(\xi-2) & -\xi(\xi-2) & -\xi^2 & \xi^2 \\ -\xi(\xi-2) & \xi(\xi-2) & \xi^2 & -\xi^2 \end{bmatrix},$$

$$\mathbf{K}_{32} = \psi_{20} \frac{\rho h}{4\tau} \frac{\partial \vartheta}{\partial x} \begin{bmatrix} \xi(\xi-2) & -\xi(\xi-2) & -\xi^2 & \xi^2 \\ \xi(\xi-2) & -\xi(\xi-2) & -\xi^2 & \xi^2 \end{bmatrix},$$

$$\mathbf{L}_{31} = \frac{\partial \beta(x,0)}{\partial x} \frac{\rho}{\tau} \psi_{20}\, \vartheta^2 \begin{bmatrix} -1 \\ 1 \end{bmatrix}, \tag{40}$$

$$\mathbf{L}_{32} = \frac{\partial \beta(x,0)}{\partial x} \frac{b\rho}{\tau} \psi_{20}\, \vartheta \frac{\partial \vartheta}{\partial x} \begin{bmatrix} 1 \\ 1 \end{bmatrix},$$

$$\mathbf{K}_{41} = \rho c_{v0} \vartheta^3 \frac{b}{6} \begin{bmatrix} -2(\xi-1) & -(\xi-1) & 2\xi & \xi \\ -(\xi-1) & -2(\xi-1) & \xi & 2\xi \end{bmatrix},$$

$$\mathbf{K}_{51} = -\psi_{20} \vartheta \rho \frac{h^2}{4\tau b} \begin{bmatrix} \xi(\xi-2) & -\xi(\xi-2) & -\xi^2 & \xi^2 \\ \xi(\xi-2) & -\xi(\xi-2) & -\xi^2 & \xi^2 \end{bmatrix} \left[\xi(\xi-2); -\xi(\xi-2); -\xi^2; \xi^2\right] \mathbf{V},$$

$$\mathbf{K}_{52} = -\psi_{20} \vartheta \rho \frac{h}{\tau} \frac{\partial \beta(x,0)}{\partial x} \begin{bmatrix} \xi(\xi-2) & -\xi(\xi-2) & -\xi^2 & \xi^2 \\ \xi(\xi-2) & -\xi(\xi-2) & -\xi^2 & \xi^2 \end{bmatrix},$$

$$\mathbf{L}_{51} = -\frac{b}{\tau} \psi_{20} \rho \vartheta \left(\frac{\partial \beta(x,0)}{\partial x}\right)^2 \begin{bmatrix} 1 \\ 1 \end{bmatrix}.$$

We can notice that $\mathbf{K}_{21}$ and $\mathbf{K}_{51}$ depend on the solution vector $\mathbf{V}$. Equation (29) is nonlinear and must be solved iteratively.

5. ARTIFICIAL DISSIPATION

Numerical damping of higher frequencies with zero damping of the basic frequency is the important question for each time integration method. Especially it can play a significant role in fast varying non linear problems. Small perturbation of the smooth solution can influence dramatically the evolution of the process. There are several papers on this subject (for example [25]). The ideal situation appears when we can control the damping properties of the procedure (in particular cases the damping should be equal to zero). Lower frequencies should not be damped while higher should be damped relatively stronger. With respect to the shape of the damping diagram we can divide all methods in two groups: the first one (Wilson, Houbolt method) with the zero slope of the damping function for small $\frac{h}{T}$, growing with the increase of $\frac{h}{T}$, and the second one (Newmark, trapezoidal rule) with a certain slope of the damping function for $\frac{h}{T} \to 0$. The practical experiences indicate that the first group damps higher modes too much, and the second group does the same with lower modes. Other methods, which use more artificial parameters in their formulations, improve the damping properties but their use is dangerous since the regular dependence of properties on the parameters does not exist.

Here, let us modify Eq. (33) by

$$\eta = 1 - \frac{\xi}{1+\gamma}, \qquad 0 \leq \gamma \leq 1. \tag{41}$$

This is the simplest way to introduce a weak numerical dissipation. For $\gamma = 0$ we have the undamped system and γ can grow till 0.05–0.1, depending on requirements. The influence of ξ and γ on the level of dissipation is shown in [8].

6. EXAMPLES

The measuring of the unitary heat, the heat conductivity coefficient (quasi-static one) and the speed of heat wave propagation, all as a function of the temperature ϑ allowed to derive and confirm the relation (1) in the form of (37) [19]. Numerical calculation is to demonstrate both the numerical method and physical behaviour of the elaborated model.

One-dimensional domain was treated for simplicity. The following values of coefficients were assumed: $\tau = 10^{-6}\,\mathrm{s}$, $L = 4\,\mathrm{mm}$, $\vartheta_0 = 1\,\mathrm{K}$, $\kappa = 500\,\mathrm{W/mK^4}$. The data were scaled to reduce the round-off errors. Then the parameters gained non-dimensional values: the length $L = 40$, mass density $\rho = 1$, material constants $c_{v0} = 0.1$, $\tau = 0.01$, $\psi_{20} = 50$. The spatial domain was divided by a uniform mesh. To the both ends no explicit boundary conditions have been imposed. However, as it has been already noticed, the assumed interpolation functions $\mathbf{N}$ allow to fulfill the Neumann homogeneous conditions on the free end, if $h \to 0$. The initial uniform temperature was $\vartheta_0 = 1(\mathrm{K})$, and the process was initiated by the initial temperature velocity jump $\dot{\beta} = 50$ put to the left end. The procedure parameter $\xi = 0.8$ has been assumed. Total time of observation was 0.05.

The first plot in Fig. 1 shows results obtained without numerical damping ($\gamma = 0.0$). 40-element mesh was used. The semi-empirical temperature is related to the initial temperature ϑ_0, for which the base of the diagram is plotted. The global solution is qualitatively changed by numerical oscillations of the solution in each time step, which are then amplified through coefficients (38) and (39). The second (Fig. 2) plot presents results obtained with damping $\gamma = 0.05$. In this case the mesh is composed of 20 spatial elements. Results prove that, while comparing with the next plot, spatial discretization is sufficient even in the case of our reduced integration of nonlinear coefficients. All the plots were smoothed by the averaging technique with 3×3 matrix. However, in the original

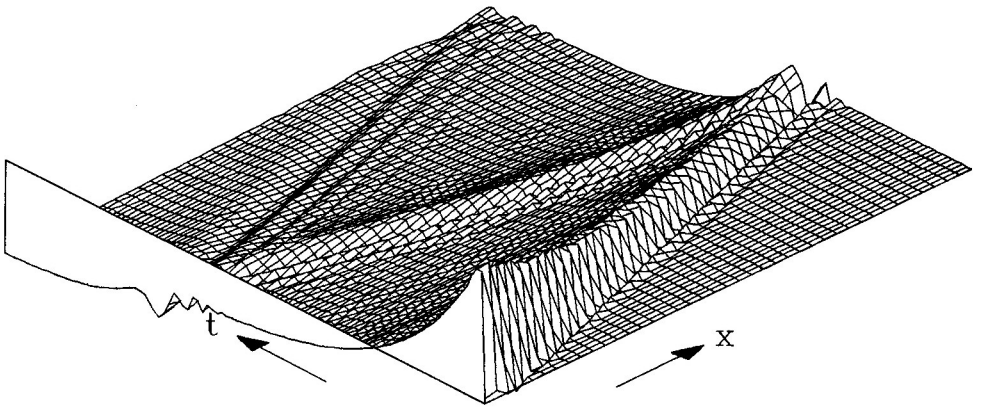

Fig. 1. Semi-empirical temperature β related to the initial temperature ϑ_0 in time without numerical damping (40 finite elements)

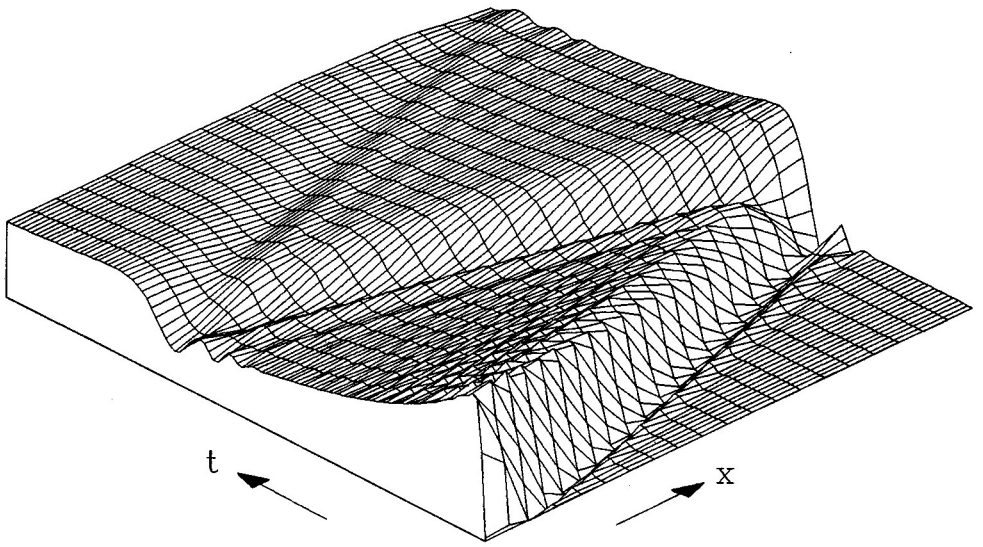

Fig. 2. Semi-empirical temperature β related to the initial temperature ϑ_0 in time with small numerical damping (20 elements)

plots we can notice high frequency spurious oscillations, visible on the left hand side of the domain in the first period of the investigation. They propagate with decreasing amplitude.

The next figure (Fig. 3) shows results obtained for our problem with 40 elements in the mesh and with numerical damping $\gamma = 0.05$. The last figure (Fig. 4) presents the shape of the peak in successive reflections from the ends of the domain. Two lines were plotted which correspond to left and right end of the domain.

7. Conclusions

The presented approach can be developed for problems discretized in a non-stationary manner. In the paper, however, we limit our analysis to a constant, uniform mesh. There is no difficulty to apply the same technique to problems with moving boundary, phase change or mesh adaptation for error reduction. The equation is strongly non-linear and the solution is sensible for disturbances of parameters. The attention should be focused on the reduction of approximation error, especially with respect to time. The efficient error estimate would be useful in an adaptive technique solution.

The example problem shows that even coarse mesh can be applied to x. The proper integration in time is essential for the convergence. It is obvious since some parameters depend on the square

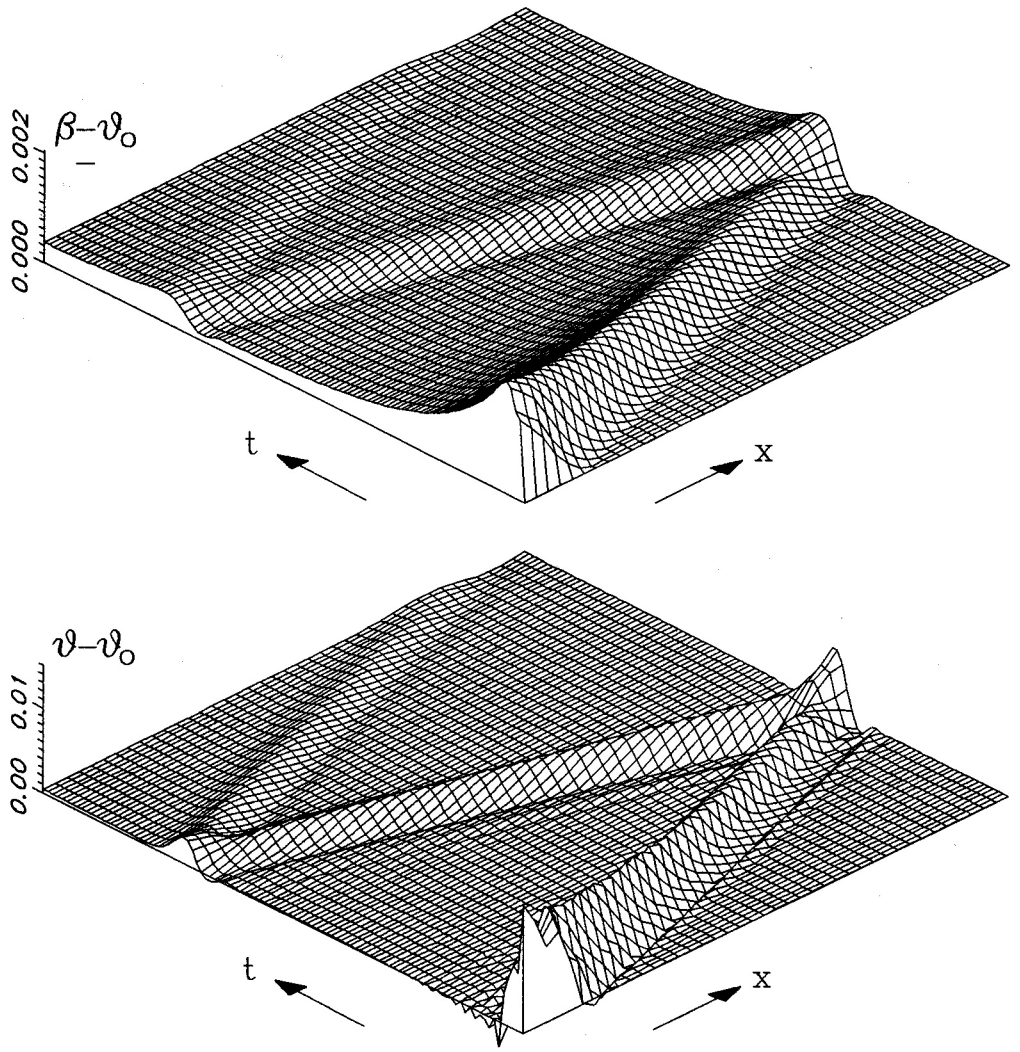

Fig. 3. Semi-empirical temperature β and real temperature ϑ in time with small numerical damping, integrated with different time step (40 finite elements)

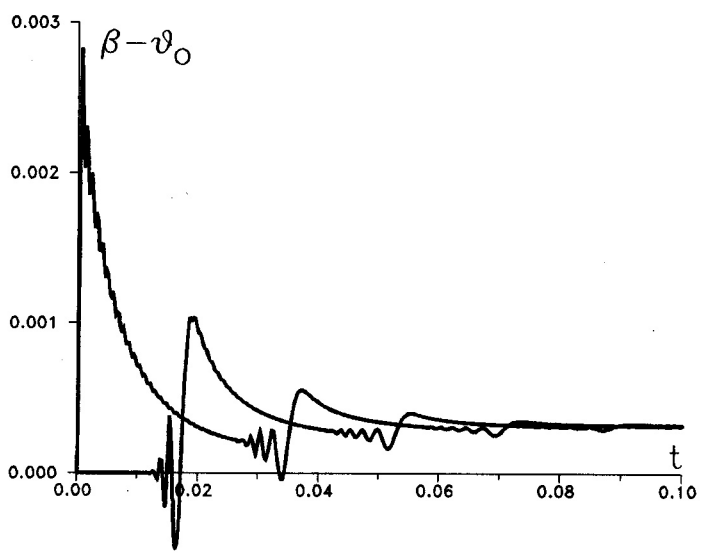

Fig. 4. The shape of the impulse during successive reflections

of the temperature rate $\dot{\beta}$. The solution of the numerical example is composed of the diffusive and wave response.

In [22] the same model equations have been analysed from the numerical point of view. There, however, different method of calculation was applied that corresponds to the finite difference method. Moreover, the authors of [22] have used slightly different constitutive function for α^*: they assumed a cubic function of ϑ. They also assumed $\vartheta = \vartheta(t, x_L)$ at one end prescribed and a homogeneous Neumann conditions at the second end. Our numerical values are very close to those assumed in [22]. The boundary condition assumed there are less physically justified from those which arrive from our interpolation functions. Consequently, in the course of the present calculations more reflections are observed at the free end as well as less attention of the wave amplitude. It seems that our numerical results are closer to experiments reported in the literature [37, 39, 40].

8. ACKNOWLEDGEMENTS

The part of the work of the second author (W. K.) has been conducted under the grant 0645/P4/93/05 from KBN (the National Scientific Research Council).

REFERENCES

[1] J.H. Argyris, D.W. Scharpf. Finite elements in time and space. *Aeron. J. Roy. Aeron. Soc.*, **73**: 1041–1044, 1969.

[2] J.H. Argyris, D.W. Scharpf. Finite elements in space and time. *Nucl. Engng. Design*, **10**: 456–469, 1969.

[3] J.H. Argyris, A.S.L. Chan. Application of the finite elements in space and time. *Ing. Archiv*, **41**: 235–257, 1972.

[4] C.I. Bajer. Triangular and tetrahedral space–time finite elements in vibration analysis. *Int. J. Numer. Meth. Engng.*, **23**: 2031–2048, 1986.

[5] C.I. Bajer. Notes on the stability of non–rectangular space–time finite elements. *Int. J. Numer. Meth. Engng.*, **24**: 1721–1739, 1987.

[6] C.I. Bajer. Adaptive mesh in dynamic problem by the space–time approach. *Comput. and Struct.*, **33**: 319–325, 1989.

[7] C. Bajer. Space–time finite element formulation for the dynamical evolutionary process. *Appl. Math. and Comp. Sci.*, **3**: 251–268, 1993.

[8] C. Bajer, R. Bogacz. New formulation of the space–time finite element method for problems of evolution. *Arch. Mech.*, **46**: 775–788, 1994.

[9] C. Bajer, R. Bogacz, C. Bonthoux. Adaptive space–time elements in the dynamic elastic–viscoplastic problem. *Comput. and Struct.*, **39**: 415–423, 1991.

[10] C. Bajer, C. Bohatier. The soft way method and the velocity formulation. *Comput. and Struct.*, **55**: 1015–1025, 1995.

[11] C. Bajer, A. Podhorecki. Space–time element method in structural dynamics. *Arch. of Mech.*, **41**: 863–889, 1989.

[12] S. Banach, S. Piekarski. Coordinate–free description of nonequilibrium thermodynamics. *Arch. Mech.*, **44**: 191–202, 1992.

[13] C. Bohatier. A large deformation formulation and solution with space–time finite elements. *Arch. Mech.*, **44**: 31–41, 1992.

[14] C. Bohatier, C. Bajer. Kinematic approach for dynamic contact problems — the geometrical soft way method. *Arch. Mech.*, **47**, 1995 (in print).

[15] C. Cattaneo. Sulla conduzione del calore. *Atti. Sem. Mat. Fis. Univ. Modena*, **3**: 83–101, 1948.

[16] C. Cattaneo. Sur une forme d'equation de la chaleur, eliminant le paradoxe d'une propagation instantaneé. *Comp. Rend. Sci.*, **247**: 431–433, 1958.

[17] M. Chester. Second sound in solids. *Phys. Rev.*, **131**: 2013–2015, 1963.

[18] V.A. Cimmelli, W. Kosiński. Nonequilibrium semi–empirical temperature in materials with thermal relaxation. *Arch. Mech.*, **43**: 753–767, 1991.

[19] V.A. Cimmelli, W. Kosiński, K. Saxton. Modified Fourier law — comparison of two approaches. *Arch. Mech.*, **44**: 409–415, 1992.

[20] V.A. Cimmelli, W. Kosiński. Well–posedness results for a nonlinear hyperbolic heat equation. *Ricerche di Matematica*, **XLII**: 1–21, 1993.

[21] I. Fried. Finite element analysis of time–dependent phenomena. *AIAA J.*, **7**: 1170–1173, 1989.

[22] K. Frischmuth, V.A. Cimmelli. Numerical reconstruction of heat pulse experiments. *Int. J. Engng. Sci.*, **33**: 209, 1995.
[23] M.E. Gurtin. Variational principles for linear initial–value problems. *Quart. Appl. Math.*, **22**: 252–256, 1964.
[24] I. Herrera, J. Bielak. A simplified version of Gurtin's variational principles. *Arch. Rat. Mech. Anal.*, **53**: 131–149, 1974.
[25] H.M. Hilber, T.J.R.Hughes, R.L. Taylor. Improved numerical dissipation for time integration algorithms in structural dynamics. *Earthquake Engng. and Struct. Dyn.*, **5**: 283–292, 1977.
[26] Z. Kacprzyk, T. Lewiński. Comparison of some numerical integration methods for the equations of motion of systems with a finite number of degrees of freedom. *Eng. Trans.*, **31**: 213–240, 1983.
[27] Z. Kączkowski. The method of finite space–time elements in dynamics of structures. *J. Tech. Phys.*, **16**: 69–84, 1975.
[28] Z. Kączkowski. General formulation of the stiffness matrix for the space–time finite elements. *Archiwum Inż. Ląd.*, **25**: 351–357, 1979.
[29] Z. Kączkowski, J. Langer. Synthesis of the space–time finite element method. *Archiwum Inż. Ląd.*, **26**: 11–17, 1980.
[30] W. Kosiński. Elastic waves in the presence of a new temperature scale. In M.F. McCarthy, M. Hayes, eds., *Elastic Wave Propagation*, 629–634. Elsevier Science (North Holland), 1989.
[31] W. Kosiński, K. Saxton. Weak discontinuity waves in materials with semi-empirical temperature scale. *Arch. Mech*, **43**: 547–559, 1991.
[32] W. Kosiński, K. Saxton. The effect on finite time breakdown due to modified fourier laws. *Quart. Appl. Math.*, **51**: 55–68, 1993.
[33] W. Kosiński, W. Wojno. Gradient generalization to internal state variable approach. *Arch. Mech.*, **47**, 1995 (in print).
[34] Z.B. Kuang, S.N. Atluri. Temperature field due to a moving heat source. *J. Appl. Mech. Trans. ASME*, **52**: 274–280, 1985.
[35] J.C. Maxwell. On the dynamical theory of gases. *Phil. Trans. Royal. Soc. London*, **157**: 49–101, 1867.
[36] A. Morro, T. Ruggeri. Second sound and internal energy in solids. *Int. J. Nonlinear Mech.*, **22**: 27–36, 1987.
[37] V. Narayanamurti, R.C. Dynes. Observation of second sound in bismuth. *Phys. Review Letters*, **28**: 1461–1465, 1972.
[38] J.T. Oden. A generalized theory of finite elements, II. Applications. *Int. J. Numer. Meth. Engng.*, **1**: 247–259, 1969.
[39] Y.M. Pao, D.K. Banerjee. Thermal pulses in dielectric crystals. *Lett. Appl. Engng. Sci.*, **1**: 33–41, 1973.
[40] T. Ruggeri, A. Muracchini, L. Seccia. Shock waves and second sound in a rigid heat conductor: a critical temperature for NaF and Bi. *Phys. Review Letters*, **64**: 2640–2643, 1990.
[41] M.P. Vernotte. Les paradoxes de l theorie continue de l'equation de la chaleur. *Comp. Rend. Sci.*, **246**: 3154–3155, 1958.
[42] P.A. Zegeling. Moving–grid methods for time–dependent partial differential equations. Technical Report 94, Centrum voor Wiskunde en Informatica, Amsterdam, 1993.